Assessment of mixture two-phase flow equations for volcanic flows using Godunov-type methods

D. Zeidan

School of Basic Sciences and Humanities
German Jordanian University, Amman, Jordan
Email: dia.zeidan@gju.edu.jo

Abstract

This paper is concerned with the numerical solution of the equations governing two-phase gas-magma mixture in the framework of thermodynamically compatible systems theory. The equations constitute a non-homogeneous system of nonlinear hyperbolic conservation laws. A total variation diminishing (TVD) slope limiter centre (SLIC) numerical scheme, based on the Riemann problem, is presented and applied for the solution of the initial boundary value problem for the equations. The model equations and the numerical methods are systematically assessed through a series of numerical test cases. Simulation results are compared and validated with different model equations available in the literature. The computed results compare well with the exact results provided for validation. Strong evidence shows that the model and the methods are accurate, robust and conservative. The model correctly describes the formation of shocks and rarefactions in two-phase gas-magma flow.

Key words: hyperbolic conservation laws; thermodynamically compatible model; volcanic eruption; compressible gas-magma; relative velocity; Godunov methods

1. Introduction

There is ongoing interest in mathematical models and computational algorithms of volcanic eruptions. A significant strand of this interest is facilitated by the spectacular natural phenomena of such volcanic processes. These processes generate a rich variety of two-phase flows depending on the geological conditions and eruptive mechanisms. In many cases, volcanic systems

develop eruptive mixtures of gas and magma into the atmosphere forming volcanic plumes [10, 12, 24]. Such activities are characterized by complex non-linear dynamics that manifest the features of unsteady two-phase flow nature. Volcanic two-phase flows are difficult to observe and they differ from other flows because of their unpredictable character. In general, studies of volcanic two-phase flows have been widely explored through theoretical and numerical modeling in analogue to available geological data and observations. Numerous authors have studied such flows as homogeneous mixture and solving the resulting governing equations like a single fluid in steady-state and transient approaches [2, 7, 14, 15, 19, 20, 22]. However, the complexity of volcanic flows has given rise to various mathematical models on the basis of currently used two-fluid models [1, 4, 8, 23]. A major disadvantage of these models is the non-conservative character of the governing equations [6, 18]. In addition to that these models are widely accepted to be ill-posed mathematically as an initial-boundary-value problem when phase velocities are unequal. However, hyperbolicity can be provided by adding stability terms such as the interfacial pressure terms and virtual mass but non-conservativity character remains in their final formulations. As a result, these models cannot be applied to non-equilibrium phenomena such as volcanic flows. Although they do provide valuable insights about non-equilibrium phenomena, they do not explicitly calculate the relative motion with transient approaches. Recently, a mathematical model has been proposed and applied to different two-phase flow problems including gas-magma mixtures [26, 27]. The model is based on the theory of thermodynamically compatible systems of hyperbolic conservation laws [5, 16, 28]. This model has three features that differentiate it from currently used models. The model is fully hyperbolic, fully conservative and allows the investigation of discontinuous solutions within two-phase flow systems by applying well-developed numerical methods of single-phase fluid dynamics. Based on current literature of volcanic processes, much important information about the non-equilibrium phenomena, wave propagation, volcanic particle aggregation and their effects, is still not fully understood. Moreover, the relative motion between phases over a wide range of velocities where phase interactions are in process is rarely investigated. A key motivation for studying this relative motion during explosive eruptions is magma fragmentation. Fragmentation plays an important role in studying such motion because of the viscosity nature of the magma involved. For instance, high viscosity magma prevents the relative velocity between the volcanic gas and magma which may result in explosive eruptions. Low vis-

cosity magmas allow for degassing and increase the effect of non-equilibrium phenomena such as the relative velocity between the two phase systems (see for instance [3] or [11] for such mechanisms and descriptions).
In this paper, we further establish and explore the fully hyperbolic and fully conservative model of [27] for volcanic flows. The model governing equations are formulated in terms of parameters of state for the mixture. It includes the balance equations of mixture mass and mixture momentum as well as necessary constitutive laws. The model also incorporates the effect of the relative motion between the phases by a kinetic constitutive equation and allows for phase interaction through such equation. In earlier work we have developed and employed the current model to predict a specific type of volcanic flow mixtures [26, 27] in which fragmentation is taking place. It is expected that the use of this mixture model will enable us not just simulate the wave structure arising from volcanic two-phase flows but also to understand the features and structures of non-equilibrium phenomena within such flows. The objective of the present study, therefore, is to continue our previous work on solving the model at hand for volcanic flow mixtures. To this end, we examine gas-magma mixture without fragmentation and with viscous phase interaction.
The outline of this paper is as follows: in the second section we describe the governing equations which make up the mixture model along with the constitutive relations used to close it. In the third section we describe the solution process to the model equations. The fourth section is devoted to the presentation and validation of the simulation results from some example computations. Finally, the fifth section gathers the main conclusions of this study.

2. Mixture two-phase flow equations

The thermodynamically compatible two-phase flow equations for mixture mass, mixture momentum and relative velocity between different phases are used to simulate the processes of interest. These equations describe the movement of volcanic gas and magma mixture with different velocities. Therefore, the utilization of a non-equilibrium model is relatively important. It is assumed that no mass transfer between both phases is considered. The differential system of balance laws for such a mixture under isentropic conditions

can be written in the following form [27, 30]:

$$\frac{\partial}{\partial t}(\rho) + \frac{\partial}{\partial x}(\rho u) = 0, \tag{1}$$

$$\frac{\partial}{\partial t}(\rho u) + \frac{\partial}{\partial x}(\rho u^2 + P + \rho c(1-c)u_r^2) = \mathcal{S} \tag{2}$$

$$\frac{\partial}{\partial t}(u_r) + \frac{\partial}{\partial x}\Big(uu_r + (1-2c)\frac{u_r^2}{2} + \psi(P)\Big) = \pi. \tag{3}$$

The symbols are standard in two-phase flow literature. ρ, ρu, P, c and u_r denote, respectively, the mixture density, mixture momentum, mixture pressure, volcanic gas mass void fraction and relative velocity between the two phase systems. These are defined as

$$\rho = \alpha\rho_2 + (1-\alpha)\rho_1 \quad \text{and} \quad \rho u = \alpha\rho_2 u_2 + (1-\alpha)\rho_1 u_1, \tag{4}$$

$$P = \alpha P_2 + (1-\alpha)P_1,\ c = \alpha\rho_2\,\rho^{-1} \quad \text{and} \quad u_r = u_2 - u_1, \tag{5}$$

where two, 2, and one, 1, are subscripts denotes the volcanic gas and magma phases, ρ_k, u_k and P_k are the density, velocity, pressure of phase k, where $k = 1, 2$, respectively, and α is the void fraction for the volcanic gas phase which is in the range $0 < \alpha < 1$. The term $\psi(P)$ appearing in (3) is given in the general form as

$$\psi(P) = e_2 + \frac{P_2}{\rho_2} - e_1 - \frac{P_1}{\rho_1} = \psi_2(P_2) - \psi_1(P_1), \tag{6}$$

which relates the two phases through the momentum equations. The phase pressures are defined by appropriate equations of stat (EOS) for each phase involved which can be written in isentropic laws as

$$P_2 = P_2(\rho_2),\ e_2 = \frac{P_2}{\rho_2(\gamma_2 - 1)} \quad \text{and} \quad e_1 = \frac{P_1}{\rho_1(\gamma_1 - 1)},\ P_1 = P_1(\rho_1). \tag{7}$$

Here γ_2 and γ_1 are are constants to be specified. It is worth pointing out that term (6) was derived and validated in [16, 17, 30] on the basis of thermodynamically compatible systems theory in terms of parameters of state for two-phase mixtures. Similar expression also was derived in [29] for gas-liquid two-phase mixtures under the assumption of mechanical equilibrium and with velocity non-equilibrium between phases. Finally, the source terms on the right-hand side of equations of (2) and (3) represent the acceleration

due to gravity g, the wall friction laws between phases and the wall as well as the conduit, respectively, and the interfacial friction laws between phases. One of the new features of the above governing equations is the inclusion of such laws in the relative velocity equation. These laws have been described by different authors in the technical literature for different real-world applications. The forms of these source terms and laws that fulfill the purpose of the current paper will be given in section 4.
The governing equations (1)-(3) can be expressed in a conservation laws form in terms of the conservative variable $\mathbb{U}$, flux $\mathbb{F}$ and source $\mathbb{S}$ vectors, respectively, as

$$\frac{\partial \mathbb{U}}{\partial t} + \frac{\partial \mathbb{F}(\mathbb{U})}{\partial x} = \mathbb{S}(\mathbb{U}), \quad t > 0, \quad x \in (-\infty, \infty), \tag{8}$$

where

$$\mathbb{U} = \begin{pmatrix} \rho \\ \rho u \\ u_r \end{pmatrix}, \mathbb{F}(\mathbb{U}) = \begin{pmatrix} \rho u \\ \rho u^2 + P + \rho c(1-c)u_r^2 \\ u u_r + (1-2c)\frac{u_r^2}{2} + \psi(P) \end{pmatrix} \quad \text{and} \quad \mathbb{S} = \begin{pmatrix} 0 \\ \mathcal{S} \\ \pi \end{pmatrix}. \tag{9}$$

With the governing equations in such form, it is clear that the system is fully conservative in terms of mixture parameters of state. Further, these equations of two-phase mixture conservation laws have a hyperbolic nature as discussed in the previous investigation. For further details to the mathematical structure and physical properties of the above equations, and comparisons with other two-phase flow models the reader is referred to [16, 30].
Altogether, equations (1)-(3) represent a system of three equations in three unknowns in terms of mixture parameters of state. The system, therefore, can be solved provided that suitable initial and boundary conditions are given. Within the context of solving system (8), a numerical approximation for a two-phase flow model that include equations for the void and mass fractions for the gas phase was presented in [27] and in [9, 17, 28, 30] for other two-phase flow applications. In addition to that, an analytical solution was also provided in [29] for a two-phase mixture model that consists of a compressible gas and incompressible liquid on the basis of the Riemann problem. The model presented in this study aims to contribute to our understanding of this important geophysical phenomenon. This simplified model

provides detailed insights into both the structure of volcanic flows and the non-equilibrium behavior within such phenomena.

3. Numerical approximation

The model equations for the one-dimensional two-phase flow of interest presented in the current paper cannot be solved analytically. This is due to the extremely high non-linearity inherent in the governing equations. Instead, a numerical approximation has been carried out on the basis of finite volume methods. Within such methods the following balance equation is derived to find the solution of system (8) at time t^{n+1}

$$\mathbb{U}_i^{n+1} = \mathbb{U}_i^n - \frac{\Delta t}{\Delta x}\left[\mathbb{F}_{i+\frac{1}{2}} - \mathbb{F}_{i-\frac{1}{2}}\right] + \Delta t\ \mathbb{S}_i. \tag{10}$$

Here Δx is the mesh spacing at time level n along with a time step Δt computed as marching in time continue. This time step is chosen according to the following formula

$$\Delta t = \text{CFL}\ \frac{\Delta x}{S_{\max}^{(n)}}, \tag{11}$$

where CFL is the Courant-Friedrichs-Lewy with $0 < \text{CFL} \leq 1$ and $S_{\max}^{(n)}$ is the maximum wave speed present throughout the computational domain at time level n. This is taken as

$$S_{\max}^{(n)} = \max_i \left\{|\lambda_i|\right\}, \tag{12}$$

for which λ_i are eigenvalues corresponding to sound waves.
In (10) $\mathbb{U}_i^n$ is an approximation to the average of the vector of conserved variables within the numerical cell, $\mathbb{F}_{i\pm\frac{1}{2}}^n$ and $\mathbb{S}_i$ are the numerical fluxes and sources. To apply (10) for solving system (8) one must replace the fluxes and sources at cell interfaces $i \pm \frac{1}{2}$ by appropriate numerical approximations. There exist various numerical methods for evaluating these numerical fluxes and sources, e.g. see [21]. For all simulations presented in this paper we use Godunov methods of centred type. These methods involve the use of the basic wave structure for the model equations when calculating the numerical fluxes appearing in (10). A Godunov centred scheme with excellent computational properties is the second-order Slope Limiter Centred

(SLIC) scheme [21]. Further, the SLIC scheme solves the homogeneous part of system (8). This homogeneous part is hyperbolic, includes discontinuities propagating into the model solution and carries information of two-phase flow variables. More specifically, the SLIC scheme can capture all these discontinuities and provide sharp resolution without spurious oscillations. For such resolutions the scheme consists of the following three steps [21]:

- Data reconstruction. In the data reconstruction step, the cell averaged values $\mathbb{U}_i^n$ are locally restored by piecewise linear function in every cell I_i as

$$\mathbb{U}_i(x) = \mathbb{U}_i^n(x) + \frac{(x - x_i)}{\Delta x}\Delta_i. \tag{13}$$

  Subsequently, the values $\mathbb{U}_i^n$ are transformed to the boundary extrapolated values as

$$\mathbb{U}_i^L = \mathbb{U}_i^n - \frac{\Delta_i}{2} \quad \text{and} \quad \mathbb{U}_i^R = \mathbb{U}_i^n + \frac{\Delta_i}{2}, \tag{14}$$

  where Δ_i defines a suitable slope limiter of the linear function set in every cell. We refer the reader to [21] for full details of available limiters.

- Evolution. The boundary extrapolated values of the previous step are evolved by a half time step, $\frac{1}{2}\Delta t$, for every cell I_i. This is carried out according to

$$\left(\mathbb{U}_i^{L,R}\right)^{\text{New}} = \mathbb{U}_i^{L,R} + \frac{1}{2}\frac{\Delta t}{\Delta x}\left[\mathbb{F}(\mathbb{U}_i^L) - \mathbb{F}(\mathbb{U}_i^R)\right]. \tag{15}$$

  The above intercell fluxes are computed at the boundary extrapolated values of every cell.

- The Riemann problem. To advance the solution in time on each cell, we solve the Riemann problem to the model equations numerically using the following standard first-order centered (FORCE) flux

$$\mathbb{F}_{i+\frac{1}{2}}^{\text{FORCE}} = \mathbb{F}_{i+\frac{1}{2}}\left(\left(\mathbb{U}_i^R\right)^{\text{New}}, \left(\mathbb{U}_{i+1}^L\right)^{\text{New}}\right), \tag{16}$$

  where $\mathbb{U}_L = \left(\mathbb{U}_i^R\right)^{\text{New}}$ and $\mathbb{U}_R = \left(\mathbb{U}_{i+1}^L\right)^{\text{New}}$. More specifically, the FORCE intercell flux is given by

$$\mathbb{F}_{i+\frac{1}{2}}^{\text{FORCE}} = \frac{1}{2}\left(\mathbb{F}_{i+\frac{1}{2}}^{\text{LF}} + \mathbb{F}_{i+\frac{1}{2}}^{\text{RI}}\right), \tag{17}$$

which is defined as the average of fluxes obtained using Lax-Friedrichs (LF) and Richtmyer (RI) methods. These are expressed as

$$\mathbb{F}^{\mathrm{LF}}_{i+\frac{1}{2}} = \frac{1}{2}\big[\mathbb{F}(\mathbb{U}^n_i) + \mathbb{F}(\mathbb{U}^n_{i+1})\big] + \frac{1}{2}\frac{\Delta x}{\Delta t}\big[\mathbb{U}^n_i - \mathbb{U}^n_{i+1}\big], \tag{18}$$

and

$$\mathbb{F}^{\mathrm{RI}}_{i+\frac{1}{2}} = \mathbb{F}(\mathbb{U}_{i+\frac{1}{2}}), \quad \mathbb{U}^{\mathrm{RI}}_{i+\frac{1}{2}} = \frac{1}{2}\big(\mathbb{U}^n_i + \mathbb{U}^n_{i+1}\big) + \frac{1}{2}\frac{\Delta t}{\Delta x}\big[\mathbb{F}(\mathbb{U}^n_i) - \mathbb{F}(\mathbb{U}^n_{i+1})\big]. \tag{19}$$

The above process provides an approximation of the local Riemann problem associated with the model equations. This solution then is used to develop the full numerical resolution across the complete wave structure.

4. Numerical tests and validations

In the following, performance of the mixture mathematical model is tested on typical explosive volcanic eruption test cases. The first test case is to numerically verify whether the model equations and the considered numerical scheme are capable of accurately determining the strong collision within volcanic tremor. The second test case is a mixture shock tube problem to test shock capturing capability of the considered scheme using the model equations. In the third test case, we simulate an expansion tube problem for a mixture of gas and magma. The last test case deals with the influence of the sources terms appearing in the model equations. Since both the volcanic gas and magma phase are considered isentropic compressible fluids, two different equations of state are employed in all simulations. Accordingly, the magma phase is assumed to be sufficiently well modeled by the stiffened equation of state given by

$$P_1 = K_1\Big(\frac{\rho_1}{\bar{\rho_1}}\Big)^{\gamma_1} - P_\infty, \tag{20}$$

where γ_1 is the ratio of specific heats of the magma, P_∞ and $\bar{\rho_1}$ are the reference pressure and density with values of 2.35, 10^5 Pa and 1.0 kg/m^3, respectively, and $K_1 = 100$ Pa. Further, the equation of state of an ideal gas is taken for the volcanic gas

$$P_2 = K_2\Big(\frac{\rho_2}{\bar{\rho_2}}\Big)^{\gamma_2}, \tag{21}$$

with the ratio of specific heats of the gas $\gamma_2 = 1.327$, $\bar{\rho_2} = 1.0\ kg/m^3$ and $K_2 = 10^5\ Pa$
In all the simulations, the initial conditions will be given along the x-space within the numerical domain $[-10, 10]$. As no exact solutions are possible for all the test cases of interest here, we calculate the reference solutions with the TVD SLIC scheme on a very fine mesh of 3000 cells. More specifically, this is regarded as a high-resolution numerical solution on a fine mesh and was checked to reliably reproduce the exact solution without the source terms. For any mesh cells used, transmissive boundary conditions, a CFL stability coefficient of 0.9 and the SUPERBEE limiter within the SLIC scheme are employed in all simulations. To check the consistency of such simulation with other studies, two set of validation calculations are carried out to confirm and judge the provided simulation results. This consideration is important, given that there are few studies found for volcanic flows using a fully compressible phases and formulation. The first validation involves a comparison of the current simulations with results provided by a commonly used numerical method, namely, the Lax-Friedrichs scheme. This scheme is explicit scheme, very straightforward, easy to apply and does not require any approximate Riemann solver. In the second set of validation, the simulations run using the exact Riemann solver of [29]. That is, we compare the simulation results provided through the model considered in this paper with analytical results obtained by a different type of an existing two-phase flow model. Further, in all the following plots, we use S model and T model labels to refer to the two-phase flow model of [29] and to the mixture model proposed in the current paper, respectively. The analytical results computed from the exact Riemann solver are found to be in close agreement in all test cases with the simulation results presented in this paper, validating both the model equations and the numerical methods employed for gas-magma mixture two-phase flow.

4.1. Gas-magma mixture collision-Volcanic tremor

In the following test case, the mixture model and SLIC scheme are investigated for an explosive eruption problem. The impact of volcanic tremor induced by magma-vapour mixture two-phase flow [4] is examined. This test consists of a very low void fraction for the gas phase, low phase densities and velocities that develop a mixture collision during an eruption. At the initial stage, the physical parameters are given by:

- Magma

$$\begin{aligned}\big(\rho_1, u_1\big)_L &= \big(958.2\ kg/m^3, \quad 1.0\ m/s\big),\\ \big(\rho_1, u_1\big)_R &= \big(958.2\ kg/m^3, -1.0\ m/s\big).\end{aligned}$$

- Gas

$$\begin{aligned}\big(\alpha, \rho_2, u_2\big)_L &= \big(0.00025, 0.598\ kg/m^3, \quad 1.0\ m/s\big),\\ \big(\alpha, \rho_2, u_2\big)_R &= \big(0.00025, 0.598\ kg/m^3, -1.0\ m/s\big),\end{aligned}$$

Figure 1 shows numerical results (symbols) of the relative velocity, mixture pressure, mixture density and mixture velocity at time $t = 0.04$. Due to tremor, the initial structure evolves into a left and right shock waves propagating in opposite direction separated by a contact discontinuity at time $t = 0.04$. The wave structure displayed in figure 1 is a typical Riemann problem for the homogenous part of system (8). In contrast, as an eruption progress mixture velocity decrease dramatically and produce large variations of the relative velocity between phases. Consequently, the relative velocity changes discontinuously across the middle wave as displayed in figure 1. In figure 1 the results (symbols) are compared against the reference solutions (solid lines) obtained by the TVD SLIC scheme on a very fine mesh of 3000 cells. All the simulations showed that the general shape of the wave structure is well captured and oscillation-free. One is also able to observe that the SLIC scheme able to achieve sharper representation of the contact discontinuity. In order to validate the results of figure 1, figure 2 show comparisons between the present simulation results with analytical solution obtained with an existing exact Riemann solver of [29]. Such a solver developed on the basis of velocity non-equilibrium of currently used two-phase flow models. Figure 2 display the relative velocity, liquid velocity, mixture velocity and mixture density at time $t = 0.04$. The solid line show the exact results and symbols represent simulations from the TVD SLIC scheme on a very fine and coarse meshes, respectively. As shown in figure 2, the results for different models and methods have the same behavior across the complete wave structure. A smooth distribution of the flow variables with both models can be seen clearly. The simulations also have the same trend as the analytical results. A discrepancy between the exact and numerical results is, however, noticeable across the contact discontinuity in the mixture density profile. This discrepancy is attributed to the inherent simplified assumptions in the exact Riemann solver associated with the model equations of [29].

4.2. Mixture shock tube problem

In order to demonstrate the ability of the mixture model and capability of the SLIC scheme for gas-magma flow simulation, the explosive volcanic eruptions test case [13, 27] is considered. The initial values as in the original problem are

- Magma

$$\begin{aligned}\big(\rho_1, u_1\big)_L &= \big(3800.0\ kg/m^3,\quad 201.0\ m/s\big),\\ \big(\rho_1, u_1\big)_R &= \big(1000.0\ kg/m^3, 201.0\ m/s\big).\end{aligned}$$

- Gas

$$\begin{aligned}\big(\alpha, \rho_2, u_2\big)_L &= \big(0.8, 10.0\ kg/m^3, 211.3\ m/s\big),\\ \big(\alpha, \rho_2, u_2\big)_R &= \big(0.8,\ \ 1.0\ kg/m^3, 211.3\ m/s\big),\end{aligned}$$

which describe a mixture of fragmented magma and exsolved volatiles at high velocities. Within the framework of two-phase flows, this is the Riemann in a shock tube with the material inside the volcanic jet modeled by the current mixture model. The simulation is performed with the TVD SLIC scheme that produces a left rarefaction wave, contact discontinuity and a right shock wave as shown in figure 3 . Figure 3 shows a comparison between the reference solution (solid lines) and approximate solutions (symbols) at time $t = 0.002$. The reference solution is carried out on a very fine mesh of 3000 cells using the TVD SLIC scheme. Whereas the approximate solutions are reproduced with the TVD SLIC, FORCE and Lax-Friedrichs methods on a coarse mesh of 100 cells at the time $t = 0.002$. The results displayed in figure 3 emphasize on the capability of both the mixture model and the SLIC scheme in the simulation of such compressible gas-magma mixture. As one can note that the plots are oscillation-free and the curves are approximating the reference solution of the Riemann problem. Further, the smearing of the contact discontinuity is clearly visible in the displayed main flow variables. The head and tail of the left rarefaction waves are accurately recovered as sharp features with the TVD SLIC scheme. From figure 3, it is easy to see that the Lax-Friedrichs scheme produces an oscillatory behavior in the relative velocity profile across the contact discontinuity. This behavior occurs with such scheme for this test case regardless of the time step and the spatial resolution.
To check the quantitative information of the provided solutions, figure 4

compares the simulation results for the same run with those obtained using the exact Riemann solver of [29]. Figure 4 gives the results of the relative velocity, mixture pressure, mixture density and mixture velocity at time $t = 0.002$. From the figure, it is easy to observe that both models have the same Riemann problem solution of this test case. There are discrepancies for the left rarefaction waves, contact discontinuities and right shock waves in comparison to the analytical solution. Examining the relative velocity results, it is observed that, the middle wave shows visible discrepancy from the analytical result. The reason for such visible discrepancy is due to the specific hyperbolicity nature of the middle wave associated with the exact Riemann solver as discussed in [29].

4.3. Gas-magma mixture expansion tube

The third test case consists of an expansion tube with a low volcanic gas volume fraction for a mixture of gas and magma. The initial conditions are [27]:

- Magma

$$\begin{aligned}\big(\rho_1, u_1\big)_L &= \big(3800.0\ kg/m^3, -500.0\ m/s\big),\\ \big(\rho_1, u_1\big)_R &= \big(3800.0\ kg/m^3, \quad 500.0\ m/s\big).\end{aligned}$$

- Gas

$$\begin{aligned}\big(\alpha, \rho_2, u_2\big)_L &= \big(0.1, 1562.0\ kg/m^3, -100.0\ m/s\big),\\ \big(\alpha, \rho_2, u_2\big)_R &= \big(0.1, 1562.0\ kg/m^3, \quad 100.0\ m/s\big).\end{aligned}$$

Three different numerical methods, namely the TVD SLIC, FORCE and Lax-Friedrichs methods are tested. The purpose here is to demonstrate that the model and methods not only behave well near sharp discontinuities but also can deal perfectly with other tube problems. Results are displayed in figure 5. The reference solution is taken to be TVD SLIC scheme with a fine mesh of 3000 cells. A comparison between simulation results (symbols) and reference solution (solid line) at time $t = 0.0015$ are depicted in figure 5 for the relative velocity, mixture pressure, mixture density and mixture velocity. The TVD SLIC scheme produces well resolved and oscillation-free solutions using a coarse mesh of 100 cells. Further, one can see clearly the three methods are in excellent agreement with the reference solutions. The difference

between simulation results is clearly observed across the contact discontinuity, head and tail of both rarefaction waves. Also, the relative velocity experience a jump across the contact discontinuity as noted in the previous test cases. The reason for this is due to the velocity non-equilibrium between the two phases.
In order to further validate this test case, we simulated the same initial conditions using the exact Riemann solver of [29]. The resulting exact and numerical simulations are compared directly in figure 6 at time $t = 0.0015$. Simulations of different models and solvers show good agreement, indicating that the current model is able to accurately predict the expansion behavior of gas-magma mixture. It is also important to note that all the previously observed discrepancies have appeared in the current test case. See the relative velocity and mixture density profiles. The comments concerning such discrepancies are equally appropriate to those of test case 4.1 and 4.2. As a result, the overall behavior as seen in figure 6 is fairly well predicted.
It is interesting to note that the simulation results for the three test cases show the same trends over the complete wave structure for the two models. This indicates that the current model is able to capture various wave observations and does not have any limitations.

4.4. Influence of the sources terms

The influence of the source terms appearing in equations (2) and (3) can be seen in figure 7. This is shown within the context of gas-magma mixture collision test case (test case 4.1). The source term in equation (2) is due to the following wall friction laws [25]

$$\mathcal{S} = -\rho g - F_{1w} \quad \text{where} \quad F_{1w} = \frac{8\mu}{r_c^2} u_1, \quad F_{2w} = 0 \quad \text{for} \quad \alpha < 0.6. \tag{22}$$

Here g, r_c, μ and u_1 are the gravity, conduit radius, the viscosity and velocity of the magma, respectively. These are constants to be specified. The above source term describes the magma before fragmentation. This is known as the Poiseuille flow where the Reynolds number for the magma is small. Further, the source term appearing in equation (3) is due to the following interfacial friction laws [25]

$$\pi = \frac{F_{1w}}{\rho_1(1-\alpha)} - \frac{3\mu}{r_b^2}\frac{\rho}{\rho_2\rho_1} u_r \quad \text{for} \quad \alpha < 0.6, \tag{23}$$

where r_b, ρ_2 and ρ_1 are the bubble radius, bubble and magma densities. These are also constants to be specified. The flow type in this case is assumed to change from the bubbly flow to the fractured-turbulent flow.
In figure 7, the same flow variables of figure 1 are displayed after the source terms effect on a CFL value of 0.001. The results are presented in the same computational domain at different magma viscosities ($\mu = 0.0000001$, 0.00001, 0.001, 1.0 $Pa\,s$) and for fixed bubble radius, r_b, of $0.01\,m$, fixed conduit radius, r_c, of $10.0\,m$ and gravity of 9.8 ms^{-2}, respectively (see [25] for further details). These values utilize the fact that the void fraction of the gas phase is very low with no fragmentation. It is worth noting that the results do not show any important change and the behavior is mainly the same after $\mu = 1.0\ Pa\,s$. One notes that the source terms of (22) and (23) have a strong effect on the complete wave structure related to the gas-magma mixture. Further, higher viscosities associated with magma are significantly influence the relative velocity profile as illustrated in figure 7. The relative velocity profile at $t = 0.04$ is magnified and redrawn in figure 8 to show its detailed structure. Figure 8 reveals that both phases will move at the same velocity when the assumption that no magma fragmentation arises while the viscosity reaches a large value. That is, the efficiency of the gas escape will increase and suppress the increase of its volume fraction accompanying the magma ascent.

5. Concluding remarks

Presented in this paper is a mixture model that has features distinct from other models used for volcanic eruptions. The model is hyperbolic, conservative and makes the use of mixture two-phase flow equations characterized by non-equilibrium phenomena of the volcanic mixture flow with a particular attention to the relative motion between phases. The model is discretized through the finite volume methods on the basis of the Riemann problem. It is shown that the mathematical model and numerical methods are able to evidence both qualitative and quantitative agreement with a broad range of test cases observed in volcanic eruptions. The mixture model with the SLIC scheme is capable of solving two-phase flow shock tube experiments with very strong discontinuities and expansion fans of the mixture mass, momentum and relative velocity in the mixture flow field. It has been noticed also that the source terms greatly affects the complete wave structure of the solu-

tion. In particular, the two phases have the same velocity when the magma viscosity increases. The simulations have been validated by comparing the results obtained with the current mixture model with different model equations available in the literature. The provided results agree well with the present simulations which validates the value of the current model equations and solutions.
Work is continuing on other aspects of two-phase flow processes in volcanic systems with the current mixture model. Future work aims to further explore in more detail the effects of magma viscosity and fragmentation on the current model equations within such systems. Further analysis may also involve turbulent drag and inertial exchange within volcanic flows on the basis of the model equations presented in this paper. Comparison model predictions with lab experiments data if possible is another future plan. Extensions to multiple dimensions are also planned on parallel implementation of the current mixture model.

Acknowledgments

A short version of this paper was presented at the 9^{th} International Symposium on Numerical Analysis of Fluid Flow and Heat Transfer - Numerical Fluids 2014 held in Rhodes, Greece, 22-28 September 2014. The author gratefully acknowledge support from the German Jordanian University.

References

[1] D. Bercovici, C. Michaut, Two-phase dynamics of volcanic eruptions: compaction, compression and the conditions for choking, Geophys. J. Int., 182 (2010) 843.

[2] M. de' Michieli Vitturi, A. Neri, T. Esposti Ongaro, S. Lo Savio, E. Boschi, Lagrangian modeling of large volcanic particles: Application to Vulcanian explosions, J. Geophys. Res. , 115 (2010) B8:8206.

[3] W. Degruyter, O. Bachmann, A. Burgisser, M. Manga, The effects of outgassing on the transition between effusive and explosive silicic eruptions, Earth. Planet. Sci. Lett., 349 (2012) 161.

[4] E. Fujita, K. Araki, K. Nagano, Volcanic tremor induced by gas-liquid two-phase flow: implications of density wave oscillation, J. Geophys. Res., 116 (2011) B09201.

[5] S.K. Godunov, E. Romenski, Elements of Continuum Mechanics and Conservation Laws, Kluwer Academic/Plenum Publishers, 2003.

[6] M. Ishii, T. Hibiki, Thermo-fluid Dynamics of Two-Phase Flow, (2nd ed.), Springer, 2011.

[7] T. Koyaguchi, An analytical study for 1-dimensional steady flow in volcanic conduits, J. Volcanol. Geotherm. Res., 143 (2005) 29.

[8] T. Koyaguchi, N.K. Mitani, A theoretical model for fragmentation of viscous bubbly magmas in shock tubes. J. Geophys. Res. 110 (2005) B10202.

[9] G. La Spina, M. de' Michieli Vitturi and E. Romenski, A compressible single-temperature conservative two-phase model with phase transitions. Int. J. Numer. Meth. Fluids, 76 (2014) 282.

[10] A. Matulka, P. López, J. M. Redondo, A. Tarquis, On the entrainment coefficient in a forced plume: quantitative effects of source parameters, Nonlin. Processes Geophys., 21 (2014) 269.

[11] A. Namiki, M. Manga, Transition between fragmentation and permeable outgassing of low viscosity magmas, J. Volcanol. Geotherm. Res., 169 (2008) 48.

[12] J.M. Oberhuber, M. Herzog, H-F. Graf, K. Schwanke, Volcanic plume simulation on large scales, J. Volcanol. Geotherm. Res., 87 (1998) 29.

[13] P. Papale, A. Neri, G. Macedonio, The role of magma composition and water content in explosive eruptions: 1. Conduit ascent dynamics J. Volcanol. Geotherm. Res., 87 (1998) 75.

[14] J.I. Ramos, One-dimensional, time-dependent, homogeneous, two-phase flow in volcanic conduits, Int. J. Numer. Meth. Fluids, 21 (1995) 253.

[15] J.I. Ramos, Two-dimensional simulations of magma ascent in volcanic conduits, Int. J. Numer. Meth. Fluids, 29 (1999) 765.

[16] E. Romenski, A.D. Resnyansky, E.F. Toro, Conservative hyperbolic formulation for compressible two-phase flow with different phase pressures and temperatures, Quart. Appl. Math. 65 (2007) 259.

[17] E. Romenski, D. Drikakis and Toro E. Conservative models and numerical methods for compressible two-phase flow. J. Sci. Comput. 42 (2010) 68.

[18] H. Städtke, Gasdynamic Aspects of Two-Phase Flow: Hyperbolicity, Wave Propagation Phenomena, and Related Numerical Methods, (1st ed.), Weinheim: Wiley-VCH, 2006.

[19] Y.J. Suzuki, T. Koyaguchi, Numerical simulations of turbulent mixing in eruption clouds, J. Earth Simulator, 8 (2007) 35.

[20] C. Textor, H-F. Graf, A. Longo, A. Neri, T. E. Ongaro, P. Papale, C. Timmreck, G.G.J. Ernst, Numerical simulation of explosive volcanic eruptions from the conduit flow to global atmospheric scales, Annals of Geophysics, 48 (2005) 817.

[21] E.F. Toro, Riemann Solvers and Numerical Methods for Fluid Dynamics: A Practical Introduction, (3rd ed.), Springer, 2009.

[22] D.L. Turcotte, H. Ockendon, J.R. Ockendon, S.J. Cowley, A mathematical model of vulcanian eruptions, Geophys. J. Int. 103 (1990) 211.

[23] A.W. Woods, A model of vulcanian explosions, Nucl. Eng. Design, 155 (1995) 345.

[24] M.J. Woodhouse, S.A. Behnke, Charge structure in volcanic plumes: a comparison of plume properties predicted by an integral plume model to observations of volcanic lightning during the 2010 eruption of Eyjafjallajökull, Iceland, Bull Volcanol, 76 (2014) 828.

[25] S. Yoshida, T. Koyaguchi, A new regime of volcanic eruption due to the relative motion between liquid and gas, J. Volcanol. Geotherm. Res. 89 (1999) 303.

[26] D. Zeidan, Drag force simulation in explosive volcanic flow, AIP Publishing, 1648 (2015) 030007-1.

[27] D. Zeidan, R. Touma, A. Slaouti, Application of a thermodynamically compatible two-phase flow model to the high-resolution simulations of compressible gas-magma flow, Int. J. Numer. Meth. Fluids, 76 (2014) 312.

[28] D. Zeidan, Numerical resolution for a compressible two-phase flow model based on the theory of thermodynamically compatible systems, Applied Mathematics and Computation, 217 (2011) 5023.

[29] D. Zeidan, The Riemann problem for a hyperbolic model of two-phase flow in conservative form, Int. J. Comput. Fluid Dynamics, 25, (2011) 299.

[30] D. Zeidan, E. Romenski, A. Slaouti E.F. Toro, Numerical study of wave propagation in compressible twophase flow, Int. J. Numer. Meth. Fluids, 54 (2007) 393.

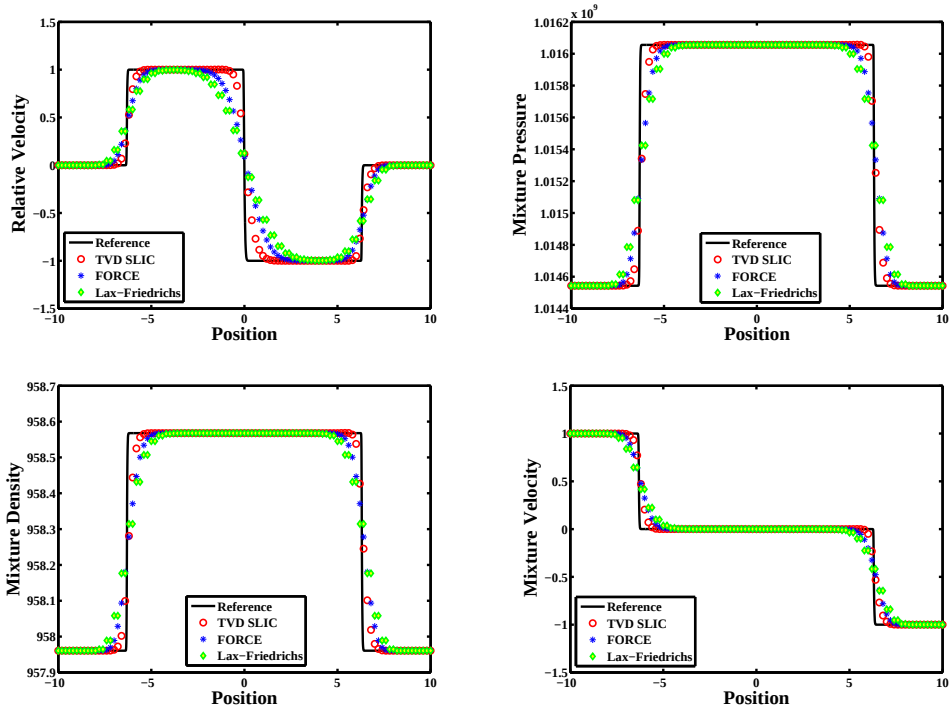

Figure 1: Gas-magma mixture collision test (test case 4.1) as computed by the TVD SLIC, FORCE and Lax-Friedrichs methods. Simulation results (symbols) are plotted at time $t = 0.04$ on 100 mesh cells with the SUPERBEE limiter along with CFL $= 0.9$. The reference solution results (solid lines) from a computation with a very fine mesh of 3000 mesh cells using the TVD SLIC scheme.

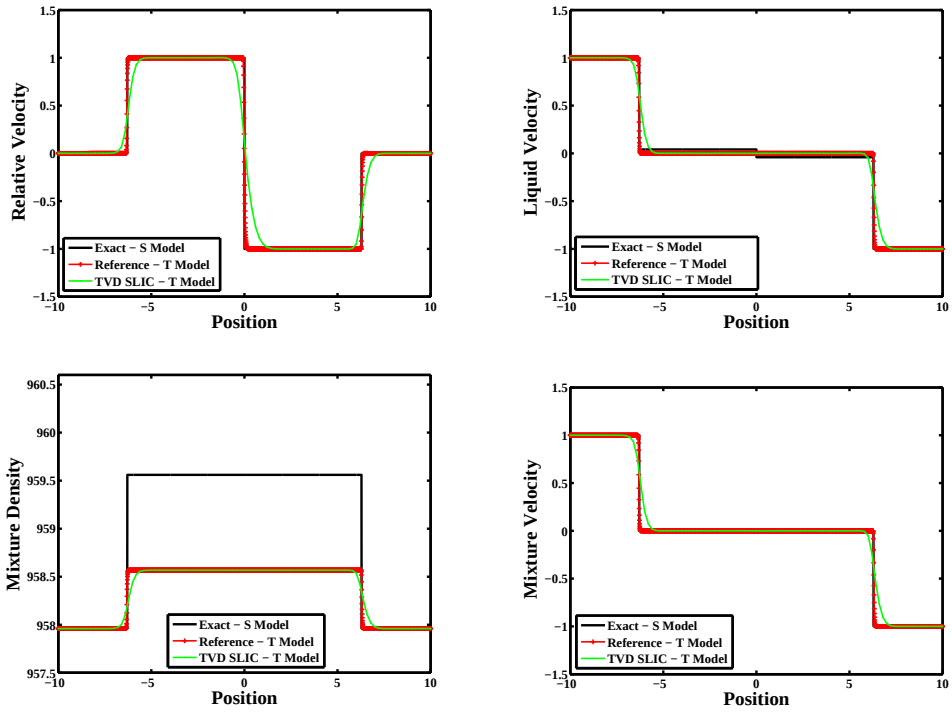

Figure 2: Comparison of numerical methods (T Model) and the exact solution (S Model) for gas-magma mixture collision test case 4.1 at time $t = 0.04$. Solid lines correspond to the exact solution while the line symbols correspond to the TVD SLIC scheme on a 3000 (red color) and 100 (green color) mesh cells, respectively, with CFL $= 0.9$.

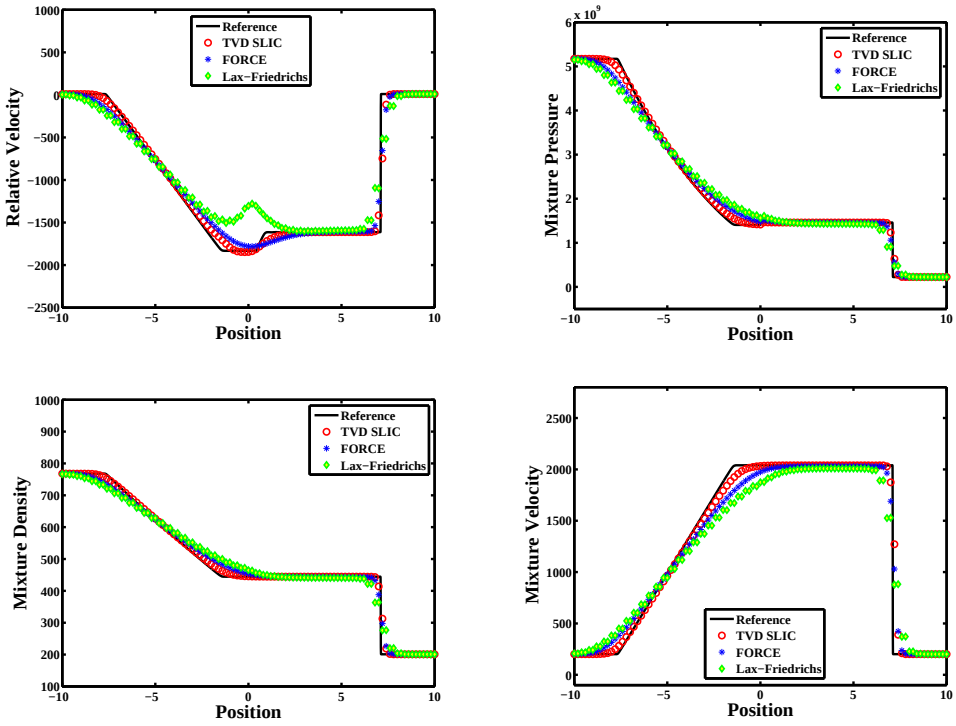

Figure 3: Mixture shock tube problem test case 4.2 at time $t = 0.002$. Simulation results (symbols) from three numerical methods (TVD SLIC, FORCE and Lax-Friedrichs) calculated on 100 mesh cells at CFL $= 0.9$ with the SUPERBEE limiter. Solid lines represent the reference solutions provided with the TVD SLIC scheme on 3000 mesh cells.

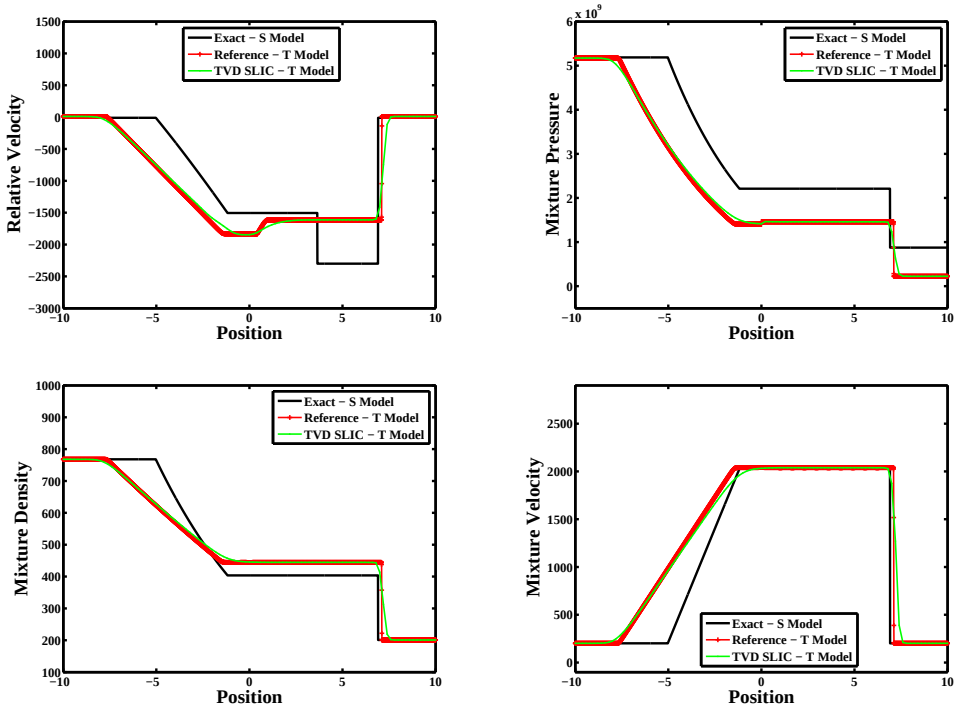

Figure 4: Exact solution and numerical approximations obtained by different solvers and models at time $t = 0.002$, test case 4.2. The solid lines indicate the exact solver of [29] while the line symbols represent the TVD SLIC scheme on 100 (green color) and 3000 (red color) mesh cells.

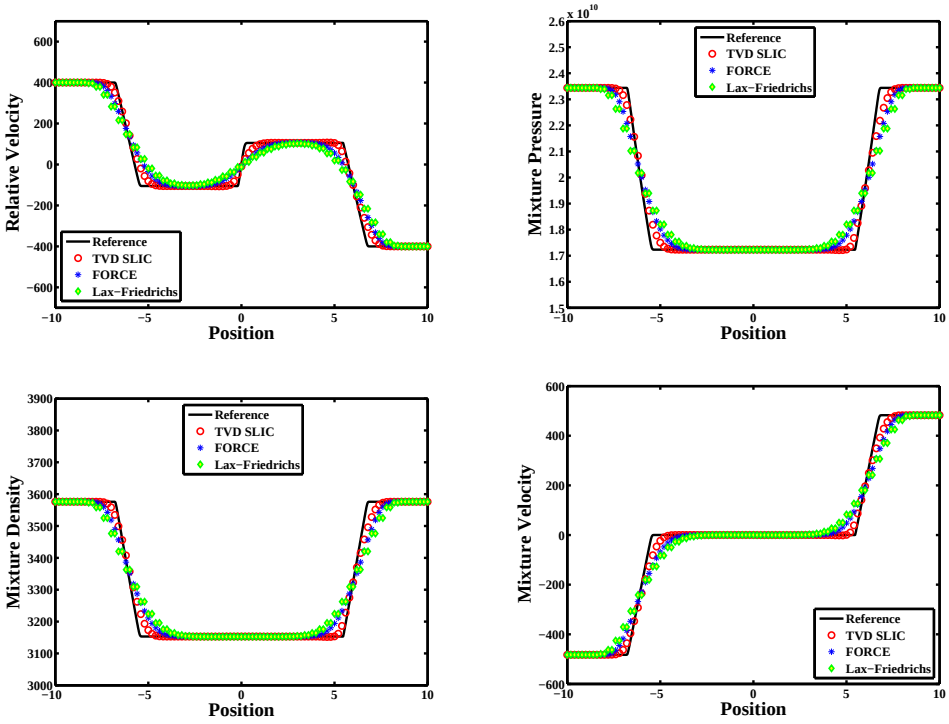

Figure 5: Simulation results for mixture expansion tube test case 4.3 with three different numerical methods, namely the TVD SLIC, FORCE and Lax-Friedrichs methods. Comparison of the numerical (symbols) and reference solutions (solid lines) is shown. These results are obtained at time $t = 0.0015$ on 100 mesh cells with a CFL value of 0.9 together with the SUPERBEE limiter.

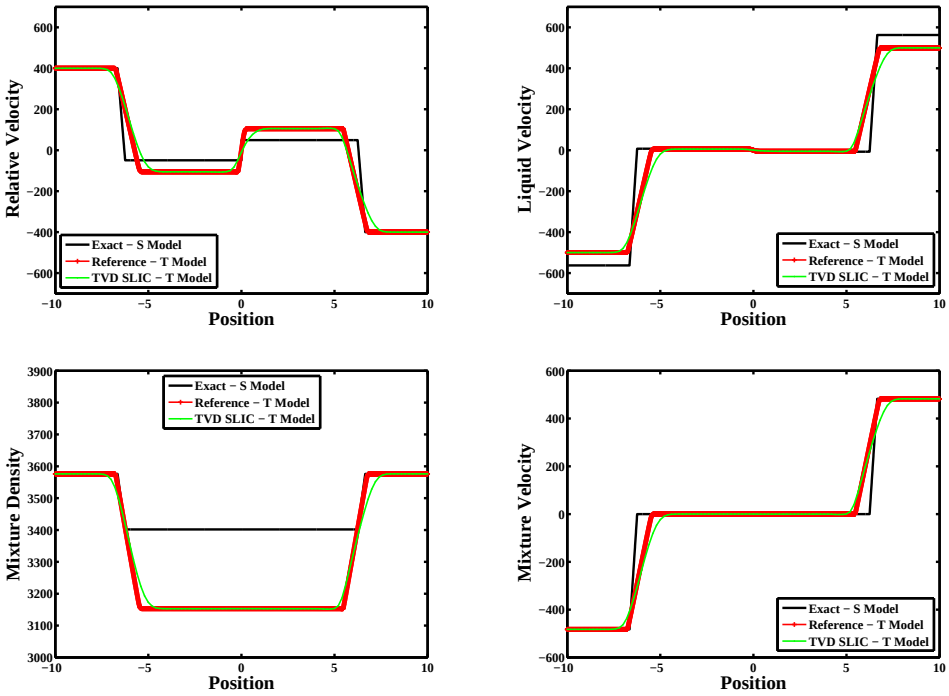

Figure 6: Flow variables for mixture expansion tube test case 4.3 on two different solvers at time $t = 0.0015$. Numerical with exact comparison. Exact solutions (solid lines) obtained with the model of [29] while the numerical resolution (symbols) with the current model and with different meshes.

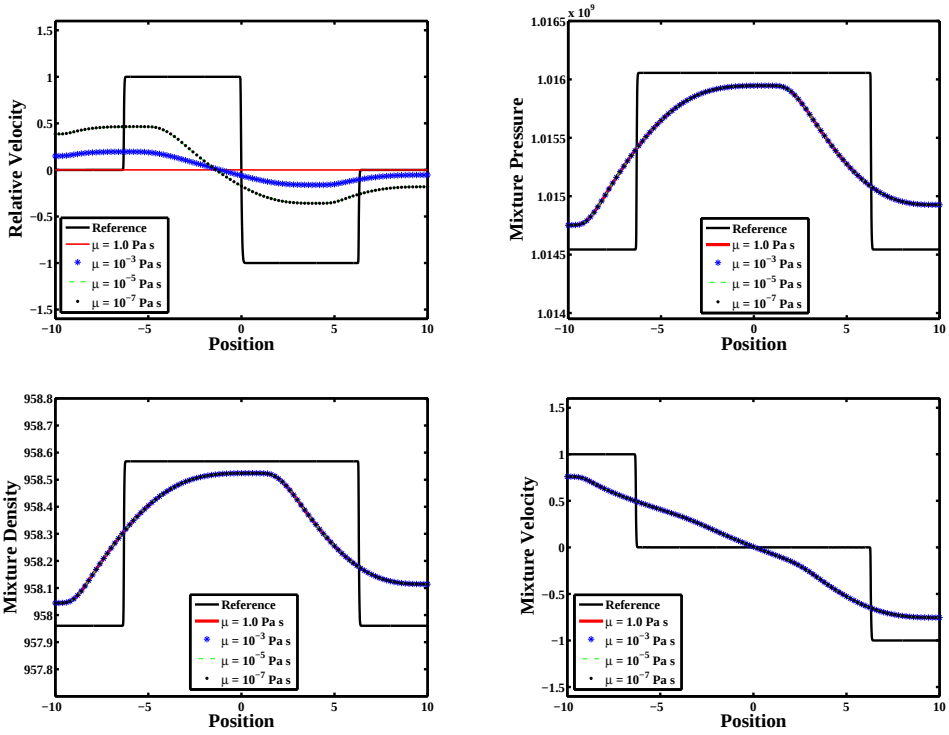

Figure 7: Effect of the source terms on gas-magma mixture collision (test case 4.1) at time $t = 0.04$. Various runs are performed to a CFL of 0.001 with μ varying from the smallest possible value of 0.0000001 to the largest possible value of 1.0.

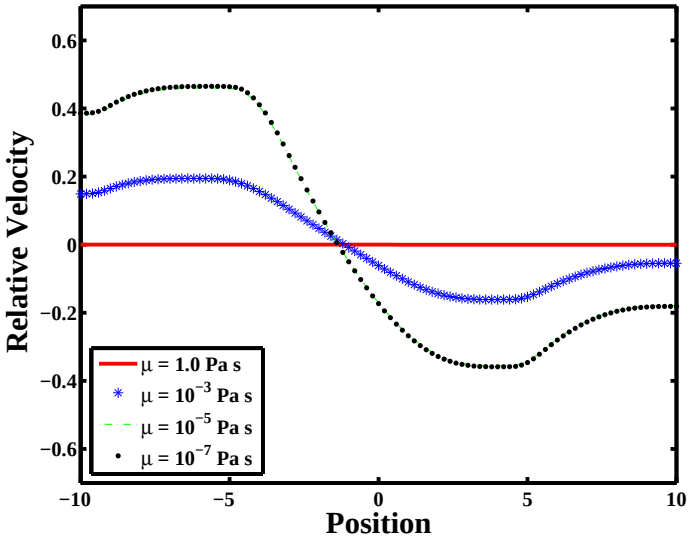

Figure 8: Effect of the highest possible value of μ on the relative velocity profile of figure 7 at time $t = 0.04$.